AFRL-AFOSR-VA-TR-2017-0104

Hollow Core Optical Fiber Gas Lasers: Toward Novel and Practical Systems in Fused Silica

Kristan Corwin
KANSAS STATE UNIVERSITY
2 FAIRCHILD HALL
MANHATTAN, KS 665061100

05/18/2017
Final Report

Air Force Research Laboratory
AF Office Of Scientific Research (AFOSR)/RTB1

REPORT DOCUMENTATION PAGE

Form Approved
OMB No. 0704-0188

1. REPORT DATE *(DD-MM-YYYY)*	2. REPORT TYPE	3. DATES COVERED *(From - To)*
18-05-2017	Final Performance	01 Nov 2013 to 31 Oct 2016

4. TITLE AND SUBTITLE
Hollow Core Optical Fiber Gas Lasers: Toward Novel and Practical Systems in Fused Silica

5a. CONTRACT NUMBER

5b. GRANT NUMBER
FA9550-14-1-0024

5c. PROGRAM ELEMENT NUMBER
61102F

6. AUTHOR(S)
Kristan Corwin

5d. PROJECT NUMBER

5e. TASK NUMBER

5f. WORK UNIT NUMBER

7. PERFORMING ORGANIZATION NAME(S) AND ADDRESS(ES)
KANSAS STATE UNIVERSITY
2 FAIRCHILD HALL
MANHATTAN, KS 665061100 US

8. PERFORMING ORGANIZATION REPORT NUMBER

9. SPONSORING/MONITORING AGENCY NAME(S) AND ADDRESS(ES)
AF Office of Scientific Research
875 N. Randolph St. Room 3112
Arlington, VA 22203

10. SPONSOR/MONITOR'S ACRONYM(S)
AFRL/AFOSR RTB1

11. SPONSOR/MONITOR'S REPORT NUMBER(S)
AFRL-AFOSR-VA-TR-2017-0104

12. DISTRIBUTION/AVAILABILITY STATEMENT
A DISTRIBUTION UNLIMITED: PB Public Release

13. SUPPLEMENTARY NOTES

14. ABSTRACT

Hollow core Optically pumped Fiber Gas LASer's (HOFGLAS's) based on population inversion combine advantages of fiber lasers such as long interaction length between pump and gas medium with those of gas lasers such as high damage threshold and substantially higher thresholds for the onset of detrimental non-linear optical effects. We have recently demonstrated the first CW HOFGLAS using molecular iodine (I2) contained in a Kagome hollow-core photonic crystal fiber (HC-PCF) as the active medium. The pump near 532 nm populated a ro-vibronic level of the first excited electronic state and lasing was observed near 1.3 m. Maximum laser output was achieved with an R=85% outcoupling mirror. A pump threshold of 7 mW corresponding to a pump intensity of about 290 W/cm2 at the fiber input was observed for optimum outcoupling. The addition of Helium buffer gas improves the lasing efficiency by a few ten percent. A phenomenological laser model can qualitatively explain the laser output power as a function of buffer gas pressure. It is a combination of pressure broadening and change of relaxation constants affecting laser saturation. The laser output mode profile suggests single-mode operation. The measured spectrum indicates lasing on multiple lines. The strongest emission originates from the terminal pump state. The lasing levels were identified using known spectroscopic data. Lasing on a single P/R doublet was observed using an intra-cavity prism as frequency selective element. The observed polarization behavior of the laser output as a function of pump polarization is likely a combination of coherent coupling from pump to laser and polarization dependent fiber properties. Preliminary experiments were performed toward simultaneous lasing in the visible and near infrared; lasing in the visible region is possible with suitable choice of cavity optics and configurations.
We are als

15. SUBJECT TERMS					
16. SECURITY CLASSIFICATION OF:			17. LIMITATION OF ABSTRACT	18. NUMBER OF PAGES	19a. NAME OF RESPONSIBLE PERSON LUGINSLAND, JOHN
a. REPORT	b. ABSTRACT	c. THIS PAGE			19b. TELEPHONE NUMBER *(Include area code)* 703-588-1775
Unclassified	Unclassified	Unclassified	UU		

A. Project Summary/Abstract

Hollow Core Optical Fiber Gas Lasers: Toward Novel and Practical Systems in Fused Silica

Final Performance Report
Submitted to: Dr. John Luginsland
Contract/Grant #: FA9550-14-1-0024

Performance Period: 11/1/2013-10/30/2016

Kristan Corwin and Brian R. Washburn, Kansas State University
Wolfgang Rudolph and Vasudevan Nampoothiri, University of New Mexico
Fetah Benabid, GPPMM group, Xlim, CNRS Research Institute, Limoges, France

Project Summary/Abstract

Abstract (>500 words)

Hollow core Optically pumped Fiber Gas LASer's (HOFGLAS's) based on population inversion combine advantages of fiber lasers such as long interaction length between pump and gas medium with those of gas lasers such as high damage threshold and substantially higher thresholds for the onset of detrimental non-linear optical effects. We have recently demonstrated the first CW HOFGLAS using molecular iodine (I_2) contained in a Kagome hollow-core photonic crystal fiber (HC-PCF) as the active medium. The pump near 532 nm populated a ro-vibronic level of the first excited electronic state and lasing was observed near 1.3 μm. Maximum laser output was achieved with an R=85% outcoupling mirror. A pump threshold of 7 mW corresponding to a pump intensity of about 290 W/cm^2 at the fiber input was observed for optimum outcoupling. The addition of Helium buffer gas improves the lasing efficiency by a few ten percent. A phenomenological laser model can qualitatively explain the laser output power as a function of buffer gas pressure. It is a combination of pressure broadening and change of relaxation constants affecting laser saturation. The laser output mode profile suggests single-mode operation. The measured spectrum indicates lasing on multiple lines. The strongest emission originates from the terminal pump state. The lasing levels were identified using known spectroscopic data. Lasing on a single P/R doublet was observed using an intra-cavity prism as frequency selective element. The observed polarization behavior of the laser output as a function of pump polarization is likely a combination of coherent coupling from pump to laser and polarization dependent fiber properties. Preliminary experiments were performed toward simultaneous lasing in the visible and near infrared; lasing in the visible region is possible with suitable choice of cavity optics and configurations.

We are also working toward a ^{13}HCN cw laser with very small quantum defect. We demonstrated the first lasers of this kind in a pulsed configuration, pumped by a ns OPA, and we have demonstrated high efficiency. Here we show the highest pulse energy to date, and also excellent beam quality as assessed with an M^2 measurement. These measurements speak well for the further power-scaling of HOFGLAS laser systems.

Motivated to achieve near-IR sources for testing fiber transmission, we have demonstrated a novel thulium/holmium fiber laser near 2 microns and systematically demonstrated optimal dispersion compensation in the fiber laser, with identification of routes toward further compensation if desired to achieve even shorter pulse durations. We have recently achieved significant dispersion compensation in the laser cavity, allowing a systematic study of the laser operation, and facilitating higher pulse bandwidths.

Finally, optical fibers for these lasers have been significantly improved during the grant period. Ultra-large band and low loss Kagome fibers that support Raman combs spanning nearly 6 octaves have been created and demonstrated, down to a wavelength of 12.7 um. A new record-low loss in Kagome lattice fiber has been demonstrated: 8 dB/km at 1 um. Furthermore, we have pushed the state-of-the art in tubular lattice fiber; a loss of 7.7 dB/km has been achieved. This is just a factor 2 above the fundamental limit of Rayleigh scattering in silica. Such fibers will continue to make new HOFGLAS systems achievable.

B. Table of Contents

C. People involved with this research grant:

C.1.1. Faculty (both tenure-track and research):

Kristan Corwin and Brian R. Washburn, Kansas State University
Wolfgang Rudolph and Vasudevan Nampoothiri, University of New Mexico
Fetah Benabid, University of Bath, then XLIM and University of Limoges, Limoges, France

C.1.2. Postdocs:

Manasadevi Thirugnanasambandam, Kansas State University

C.1.3. Graduate students:

Neda Dadashzadeh, Kansas State University, Ph.D. candidate
Kushan Weerasinghe, Kansas State University, Ph.D. candidate
Rajesh Kadel, Kansas State University, Ph. D. 2014
Esmaeil Souchelmaei, University of New Mexico, Ph.D. candidate
Farzin Aghbolagh, University of New Mexico, Ph.D. candidate

C.1.4. Engineers

Martin Maurel, Xlim
Matthieu Chafer, Xlim

D. Archival publications and patents (published) during reporting period:

1. B. Debord, A. Amsanpally, M. Chafer, A. Baz, M. Maurel, J.-M. Blondy, E. Hugonnot, F. Schol, Vincetti, F. Gérôme, and F. Benabid, "Ultralow transmission loss in inhibited-coupling guiding hollow fibers," Optica, *accepted* (2017).
2. DEBORD B., MAUREL M., AMSANPALLY A., ADNAN M., BEAUDOU B., BLONDY J.-M., VINCETTI L., GÉRÔME F., BENABID F.: "Ultra-low loss (8.5 dB/km @ Yb-laser region) inhibited-coupling Kagome HC-PCF for laser beam delivery applications" , Photonic West, Paper 10094-58, San Francisco, California, 28 January - 2 February 2017 *accepted*.
3. N. Dadashzadeh, M. Thirugnanasambandam, K. Weerasinghe, B. Debord, M. Chafer, F. Gérôme, F. Benabid, B. Washburn, and K. Corwin, "Power-scaling a Mid-IR OPA-pumped Acetylene-filled Hollow-Core Photonic Crystal Fiber Laser," in *Conference on Lasers and Electro-Optics*, OSA Technical Digest (2016) (Optical Society of America, 2016), paper STh4O.1. https://doi.org/10.1364/CLEO_SI.2016.STh4O.1
4. N. Dadashzadeh, M. Thirugnanasambandam, K. Weerasinghe, B. Debord, M. Chafer, F. Gérôme, F. Benabid, B. Washburn, and K. L. Corwin, "Near-Gaussian Spatial Mode from a Mid-IR Acetylene-filled Hollow-Core Fiber Laser," in *Frontiers in Optics 2016*, OSA Technical Digest (online) (Optical Society of America, 2016), paper FTu1I.5. https://doi.org/10.1364/FIO.2016.FTu1I.5
5. A. V. V. Nampoothiri, B. Debord, M. Alharbi, F. Gérôme, F. Benabid, and W. Rudolph, "CW Hollow Core Optically Pumped I_2 Fiber Gas Laser," Opt. Lett. **40**, 605-608 (2015). doi:10.1364/OL.40.000605
6. R. Kadel and B. R. Washburn, "Stretched-Pulse and Solitonic Operation of an All-Fiber Thulium/Holmium Doped Fiber Laser," Appl. Opt. **54**, 746-750 (2015). https://doi.org/10.1364/AO.54.000746
7. A. Benoit, B. Beaudou, M. Alharbi, B. Debord, F. Gerome, F. Salin, and F. Benabid, " Over-five octaves wide Raman combs in high-power picosecond-laser pumped H_2-filled inhibited-coupling Kagome fiber", Optics Express **23**(11) 14002-14009 (2015). https://doi.org/10.1364/OE.23.014002
8. N. Dadashzadeh, K. Weerasinghe, A. Jones, B. Debord, F. Gerome, F. Benabid, B. Washburn, and K. Corwin, "Mode Profile of a Mid-IR Gas-filled Hollow-Core Photonic Crystal Fiber Laser," in *Frontiers in Optics 2015*, OSA Technical Digest (online) (Optical Society of America, 2015), paper LTh4I.4. https://doi.org/10.1364/LS.2015.LTh4I.4

9. Wolfgang Rudolph, Amarin Ratanavis, Vasudevan Nampoothiri, Kristan L. Corwin, Andrew M. Jones, Rajesh Kadel, Brian R. Washburn, Rajesh Kadel, and John M. Zavada, "Gas Filled Hollow Fiber Laser," U.S. Patent Number **US 9,106,055**, (2015).
10. Rajesh Kadel, Ph.D. Thesis, Laser dynamics of a mode-locked thulium/holmium fiber laser in the solitonic and the stretched pulse regimes, Kansas State University (201**4**) http://krex.k-state.edu/dspace/handle/2097/17556
11. V. A. Nampoothiri, W. Rudolph, B. Debord, M. M. Alharbi, F. Gérôme, and F. Benabid, "CW Hollow Core Optically Pumped Fiber Gas Laser," in CLEO: 2014, OSA Technical Digest (online) (Optical Society of America, 2014), paper SM3N.3. http://www.opticsinfobase.org/abstract.cfm?URI=CLEO_SI-2014-SM3N.3

D.1. Papers submitted or in preparation:

1. N. Dadashzadeh, M. P. Thirugnanasambandam, K. Weerasinghe, B. Debord, M. Chafer, F. Gerome, F. Benabid, B. R. Washburn and K. L. Corwin, "High energy, near diffraction-limited performance of OPA pumped Acetylene-filled Hollow-core Optical Fiber Gas Laser in mid-IR," *in preparation.*

The following papers are related to the project, and the results of them will strengthen the project, but were not directly funded by the AFOSR grant:

1. A. Benoit, B. Beaudou, M. Alharbi, B. Debord, F. Gerome, F. Salin, and F. Benabid, "Generation of Raman comb over two octaves with picosecond pulse laser in hydrogen-filled Kagome HC-PCF," in *CLEO: 2014*, OSA Technical Digest (online) (Optical Society of America, 2014), paper SM3N.2. http://www.opticsinfobase.org/abstract.cfm?URI=CLEO_SI-2014-SM3N.2

D.2. Abstract of Ph.D. Thesis by Rajesh Kadel (item [2] above):

Mode-locked lasers that produce short optical pulses in the mid-infrared wavelength region have been sought out for a wide range of applications such as free space communication, molecular spectroscopy, medical diagnostics, and remote sensing. Here, a thulium and holmium (Tm/Ho) co-doped fiber laser that mode-locks in both the solitonic and stretched-pulse regimes is used to produce ultra-short pulses in the 2 μm region. Nonlinear polarization rotation technique is used where fiber nonlinearity is responsible to mode-lock the laser. The anomalous group velocity dispersion of both the single mode and gain fibers used limit the laser operation in the solitonic regime where the spectral bandwidth is 10 nm and hence the pulse duration is limited to 996 fs. In order to increase the spectral bandwidth and hence get the shorter pulses the anomalous dispersion of these fibers has to be compensated using normal group velocity dispersion fiber in the laser cavity.

High numerical aperture fibers, which have normal group velocity dispersion around 2 μm due to its large and positive waveguide dispersion, can be used to compensate the anomalous dispersion of the gain and single mode fibers. We used a high numerical aperture fiber called UHNA4 in the laser cavity in order to compensate the anomalous dispersion of other fibers and mode-locked the laser in stretched pulse regime. The spectral bandwidth of the laser increased to 31 nm with corresponding pulse duration of 450 fs measured from the interferometric autocorrelation. The laser dynamics of the Tm/Ho co-doped fiber laser is also studied while going from the stretched-pulse to solitonic regime by fiber cut-back measurements of normal dispersion fiber. It was clearly observed that both the spectral bandwidth and the pulse duration changed significantly going from one region to the other.

E. Summary of Important Results

E.1. Molecular Iodine Laser, University of New Mexico

The following tasks were performed during the performance period of the project:

1) First demonstration of cw lasing in a Hollow Core Photonic Crystal Fiber, using molecular Iodine (I_2) as the active medium.
2) Characterization of the cw I_2 hollow core fiber gas laser (HOFGLAS); effect of the outcoupler and buffer gas pressure.
3) Polarization coupling of pump and laser radiation of cw I_2 HOFGLAS.
4) Exploring possibility of simultaneous lasing in the visible (540-700nm) and near-IR (1.3 μm) regions in I_2 HOFGLAS.

We have demonstrated cw lasing in an Iodine (I_2) filled ~85-μm hollow core photonic crystal fiber when optically pumped at 532 nm. [1,2] This is the first demonstration of a cw Hollow Core Optically pumped Fiber Gas Laser. The setup of the cw HOFGLAS is shown in Fig. 5. The output from a single-frequency, tunable (over ~8 GHz), 532-nm cw Nd:YVO4 laser was expanded, collimated and focused onto the input facet of a ~20-cm long HC-PCF fiber. The fiber was contained in a I_2 gas cell. The measurements were carried out at room temperature, the I_2 pressure was approximately 300 mtorr of I_2 (vapor pressure of I_2 at room temperature).

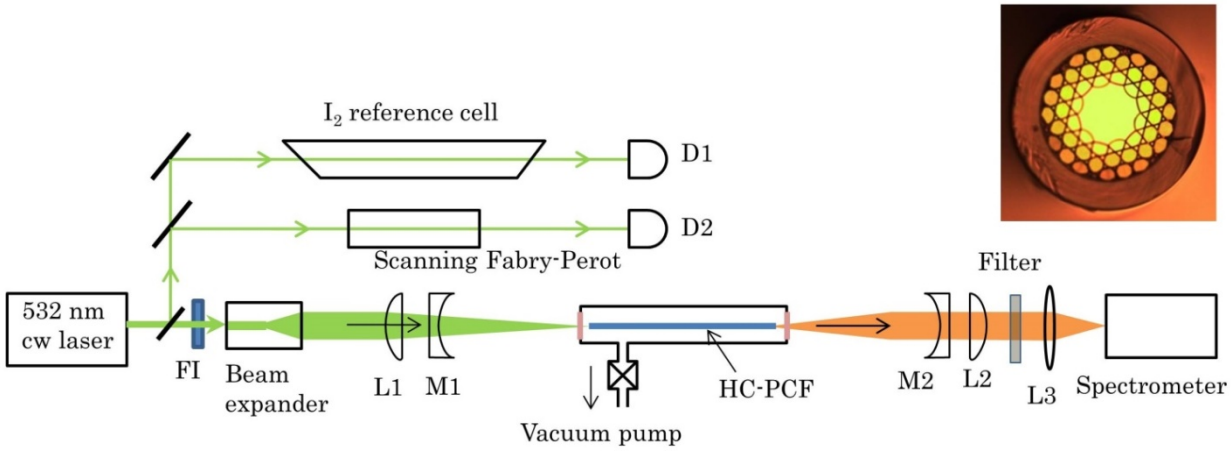

Fig. 1 Hollow Fiber Gas LASer (HOFGLAS) setup. The fiber is filled with molecular iodine, I_2, and pumped at 532.1 nm using a tunable CW Nd:Vanadate laser (Coherent, Verdi). L1 is input coupling lens, focal length and position chosen so as to have optimum input coupling. Curved mirrors M1, M2 form the fiber laser resonator cavity. FI- Faraday isolator; L2, and L3 are lenses used for focusing/collimation. The cross-section of the kagome Hollow Core Photonic Crystal Fiber (HC-PCF) used in the experiment is shown on the upper right corner. The fiber was provided by F. Benabid and co-workers from Xlim Research Institute, France.

The ends of the gas cell were sealed with windows antireflection coated for both pump and lasing wavelengths. The output from a tunable (over ~8 GHz around 532.1 nm), single-frequency, frequency doubled CW Nd:YVO4 laser was expanded, collimated and focused onto the input facet of the hollow core fiber. The frequency stability and single-frequency operation of the pump laser were ensured by monitoring pump absorption through a 10-cm long reference I_2 cell (300 mtorr) and a scanning Fabry-Perot interferometer, respectively. Iodine was pumped on one of the rotational-vibrational lines on its $v'' = 0 \rightarrow v' = 32$ of the $B^3\Pi^+_{0u} \leftarrow X^1\Sigma^+_g$ electronic transition near 532 nm.

A hollow photonic crystal fiber having a hypocycloid contour core with a core diameter of ~85 μm was used in the experiment. The normalized transmission spectrum of the fiber is shown in Fig. **Error! Bookmark not defined.**. The fiber had a low-loss of ~30 dB/km at our laser emission wavelength range of 1200-1350 nm.

A loss of about 42 dB/m at the pump wavelength of 532nm was estimated by measuring the pump transmission coefficient before filling in the gas and assuming a coupling efficiency of 100%. The small signal absorption of the pump in the I_2 filled HC-PCF was approximately 99.5%.

The cavity consisted of two focusing mirrors of radius of curvature 15-cm with one of the mirrors (M1) having high reflectivity at the expected laser wavelength and an outcoupler mirror (M2) with partial transmission at the lasing wavelength. Both mirrors had high transmission at the pump wavelength. Outcoupling mirror reflectivities from 55% to 99% were used in the experiments. For a few outcoupling values, an antireflection coated lens of focal length 15 cm and a plane mirror of suitable reflectivity was used as a substitute to the curved mirror outcoupler. Since the position of the mirrors is critical, the initial positions and alignment of the cavity mirrors were optimized

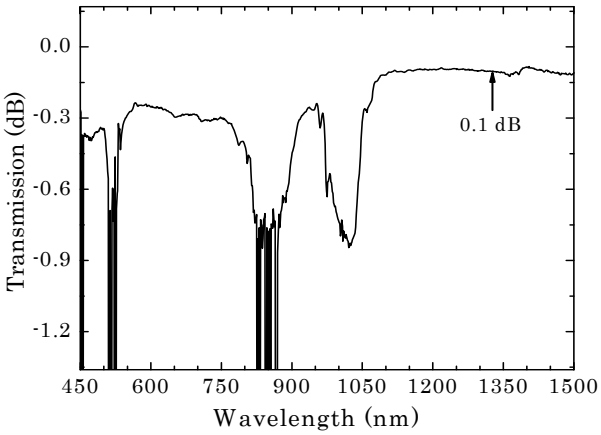

Fig. 2: Normalized (to source) transmission of a 3-m long HC-PCF (curve provided by Dr. Fetah Benabid, Xlim Research Institute).

by minimizing the round trip loss of a diode probe laser propagated through the fiber. The latter were found to be as low as 0.5%.

A laser threshold of less than 5 mW of input power at the input of the fiber (the actual power coupled into the fiber is even lower) was observed. The laser threshold for various outcoupler reflectivities is shown in Fig. 3.

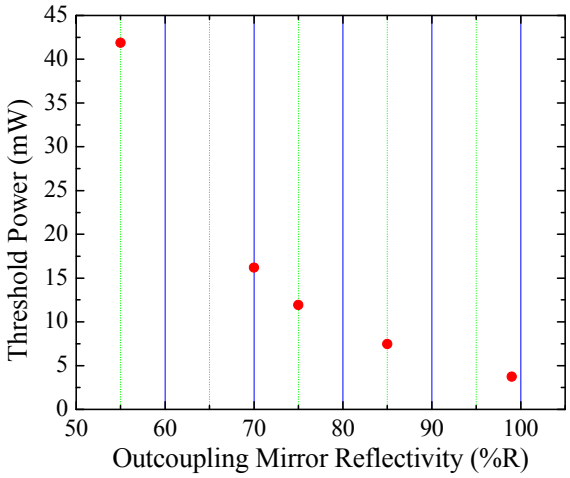

Fig. 3: Threshold input power as a function of outcoupling mirror reflectivity.

Laser output from the I_2 HOFGLAS at a pump power of 140 mW as a function of various outcoupling reflectivity is shown in Fig. 4. The pump laser was tuned to the P (50) line of the $B^3\Pi^+_{0u}$ ($v' = 32$) ← $X^1\Sigma^+_g$ ($v'' = 0$) absorption transition. As can be seen, for the R = 85% outcoupler the laser output power reaches a maximum. Note, the total outcoupling loss was about 22% taking into account passive losses from the cell windows (~ 7%). At this value of

outcoupling, the pump threshold for lasing was 7 mW, which corresponded to a pump intensity of approximately 290 W/cm^2.

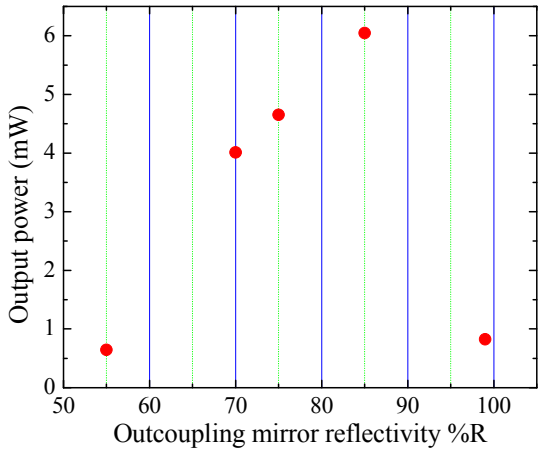

Fig. 4 Laser output power as a function of outcoupler reflectivity recorded for an input pump power of 140 mW.

Figure 5 shows the laser spectrum for an input pump power of 140 mW (R = 85%). Also shown to the right is a simplified energy level diagram of I_2 with the relevant transitions. All observed lasing lines originate from the terminal pumped state. There are three lasing transitions in the 1.3 μm region; each transition is a doublet with corresponding R and P branches. From the known spectroscopic constants, the transitions are identified as R (48) and P (50) transitions from the pumped (v′ = 32) level to v″ = 72, 71, and 69 levels. The vibrational quantum numbers of the lower laser levels are determined by a combination of the spectral filter provided by the passive cavity and the Franck-Condon factors in this spectral region.

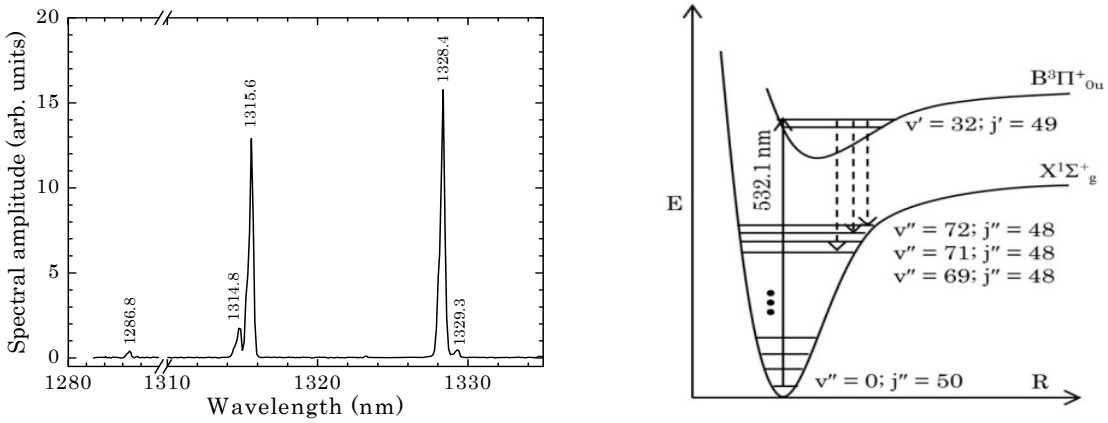

Fig. 5 (Left) Spectrum of laser recorded with R=85% outcoupler and (Right) a simplified energy level diagram of I_2 indicating pump and relevant laser transitions. Pump power was 140 mW.

I_2 HOFGLAS output power as a function of input power for different outcoupler reflectivities is shown in Fig. 6. Initially the laser output varies linearly with input pump power before it starts to level-off at higher input powers. The latter is likely due to saturation of the pump transition and a reduction in gain due to dissociation of I_2 from the upper and lower laser levels (v″ = 72). These levels are close (within 6 k_BT) to the dissociation energy.

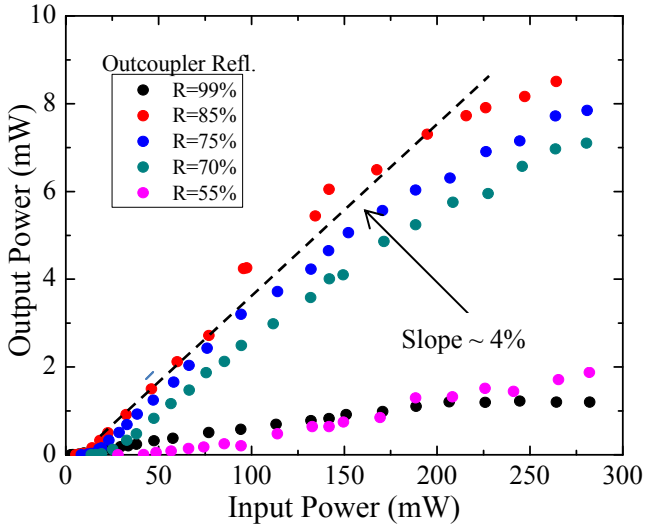

Fig. 6**:** I_2 HOFGLAS output power as a function of input power for various outcouplers.

From Fig. 6, it also can be seen that the levelling off of the laser output occurs at much lower power for R=99% compared to eg, R=55% where no "saturation" is observed even at the maximum pump power. The apparent early "saturation" behavior at higher output coupler reflectivities could be attributed to relatively larger intracavity circulating power. The data show deviation from the linear behavior for all but the 55% mirror. These occur roughly at the same input power. A maximum multiline output of about 8 mW was obtained for about 270 mW of pump power. Using the 85% reflectivity outcoupler, a maximum slope efficiency of ~4% was achieved from this HOFGLAS. CW laser action lasting for several hours was observed without any degradation in performance.

Laser output spatial profile

I_2 HOFGLAS beam profile recorded by scanning a 1-D (linear) InGaAs array across the laser output is shown in Fig. 7. In this case, the outcoupler consisted of a lens - plane mirror combination producing collimated output. The vertical (y) and horizontal (x) line profiles along with corresponding Gaussian fit are also shown. The beam profile is slightly elliptical with radii ($1/e^2$ Intensity) ~2.8 mm and 2.6 mm, respectively; the small ellipticity could be arising due to slight misalignment of intra-cavity lens which forms the part of outcoupler. Overall, the beam profile suggests that lasing produces a single spatial mode.

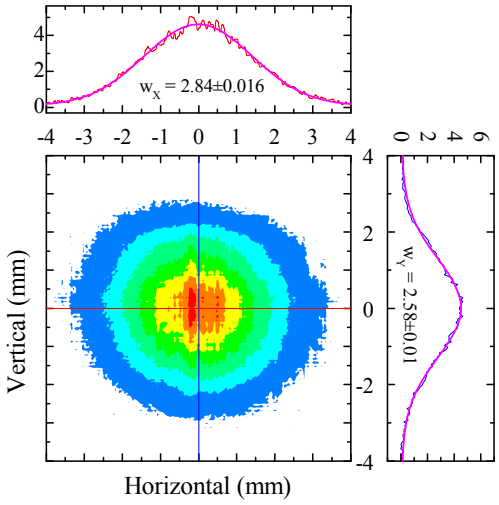

Fig. 7 I_2 HOFGLAS beam profile.

Buffer gas dependence on laser performance

In order to study effects of buffer gases on laser efficiency, we have carried out measurements on laser output with addition of buffer gas (Helium) to I_2. The I_2 pressure was kept constant at 300 mtorr. For a constant input power of ~ 70 mW, laser and residual pump transmission were recorded for various buffer gas pressures. Laser and transmitted (residual) pump output as a function of buffer gas pressure for two outcouplers, R=90% and R=99%, are shown in Fig. 8(a). The curves are normalized to their respective peak values. The laser absorption increases with addition of buffer gas. Also, laser output first increases and then rolls over rapidly for buffer gas pressures above ~ 1 torr. This behavior can be understood in terms of interplay of two phenomena caused by collisions of I_2 molecules with buffer gas; (i) increasing saturation intensity of the laser transition, and (ii) reduced small signal gain coefficient due to pressure broadening. A simple phenomenological laser model can be used to explain the observed behavior qualitatively. Laser output dependence on saturation intensity and gain can be expressed as

$$I_0 = I_s\left(\frac{\gamma_0}{\ln\left(\frac{1}{R}\right)} - 1\right), \qquad (1)$$

where I_s is the saturation intensity, R is the outcoupler reflectivity, and γ_0 is the small-signal gain. The pressure dependence of saturation intensity and gain coefficient can be expressed as $I_s = \bar{I_s}(1 + a_1 p)$, and $\gamma_0 = \bar{\gamma_0}/(1 + a_2 p)$ respectively, where $\bar{I_s}$, a_1, and a_2 are phenomenological constants, p is the buffer gas pressure, and $\bar{\gamma_0}$ is the unsaturated gain coefficient. Figure 8(b) shows the laser output as a function of buffer gas pressure using the above equation. It is evident that the model qualitatively predicts the observed trend in Fig. 8(a). In our case, the addition of Helium results in faster relaxation out of the lower laser state, thus increasing saturation intensity. As a result, we see an increased absorption initially and increased laser gain.

The absorption will continue increasing with addition of Helium till reaching the linear absorption regime at about 1 torr of Helium. Any further addition of buffer gas will not contribute to absorption; rather it will deplete the population (gain) at the upper laser level available for stimulated emission, reducing the lasing efficiency.

There are two competing channels for the reduction of upper laser state population: buffer gas induced collisional removal as well as stimulated emission. Because of larger intracavity power, the stimulated emission rate is higher in case of R=99% compared to R=90% outcoupler- hence the former is less affected with depopulation of upper laser level by buffer gas. This is clearly reflected in the slower slope for the R=99% laser output curve beyond 1 torr.

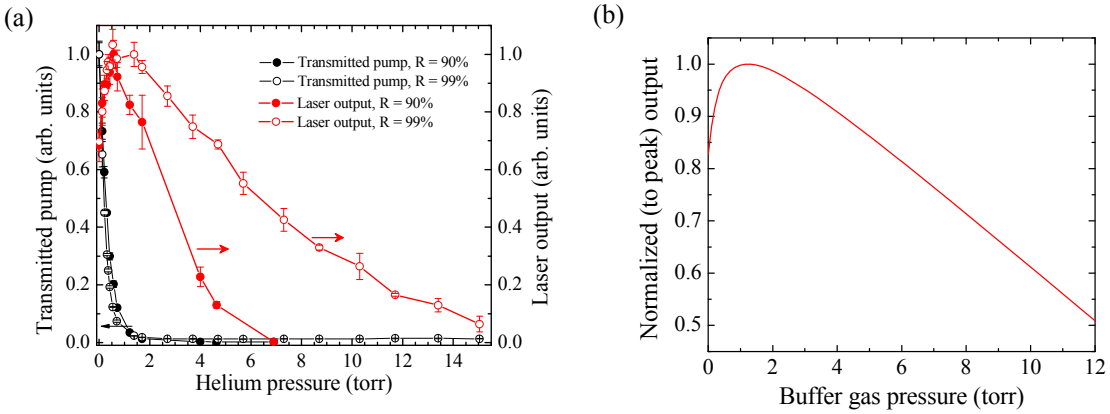

Fig. 8 (a) Laser output (right axis) and transmitted pump (left axis) as a function of buffer gas pressure, shown for two values of outcouplers, (b) Laser output as a function of buffer pressure, predicted by the phenomenological model. All curves are normalized to their respective peak values.

Figure 9 shows the laser output power dependence obtained as a function of pump power for two buffer gases, Helium and CO_2. The buffer gas pressure was kept around 1 torr (near the optimum for maximum laser power). The outcoupler reflectivity was 85%. It can be seen that CO_2 has a stronger effect on laser efficiency compared to Helium. This could be due to CO_2 having more degrees of freedom increasing cross sections for inelastic collisions. The addition of buffer gases didn't give rise to new laser components. However, it was noted that, for the weaker lines it was possible to achieve either lase only on one R or P component completely suppressing the other component by careful cavity alignment.

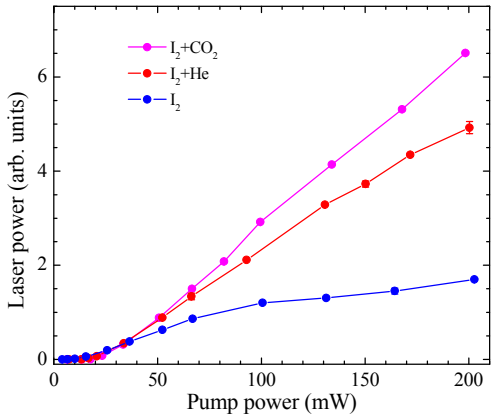

Fig. 9 Laser output power as a function of input pump with the addition of buffer gases Helium and CO_2. Also shown the output without addition of any buffer gas.

Wavelength selection using intra-cavity prism

In order to selectively enable/suppress various wavelength components, a sapphire prism was inserted in the cavity. Figure 10(a) shows the setup. A resonator built with a high reflector mirror M1 and a lens (f=15 cm)/plane mirror (M2, R=85%) combination formed the outcoupler. For these experiments, I_2 was pumped on the P47 ($v''=0 \rightarrow v' = 32$) transition near 532 nm. The laser spectrum with and without prism is shown in Fig. 10(b). The use of an intra-cavity prism enables to select lasing in a wavelength window of about 1 nm. Since the monochromator resolution is limited (0.5 nm), in order to resolve the features within the two lines selected by the prism, the laser output was sent to a high resolution (7.5 GHz) Optical Spectrum Analyzer (OSA).

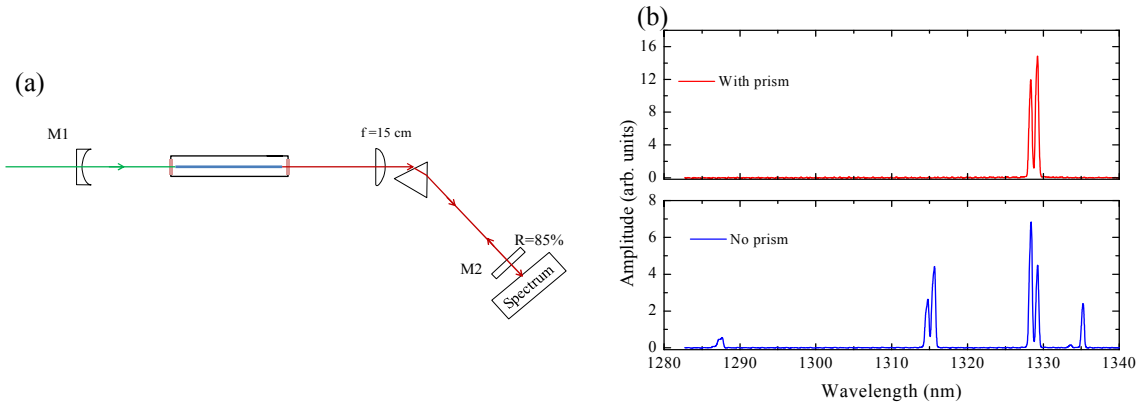

Fig. 10 (a) Experimental setup for wavelength selection from I_2 HOFGLAS using an intra-cavity prism, and (b) laser spectrum with and without intra-cavity prism (resolution of spectrometer ~ 0.5 nm).

Figure 11 shows spectral features of the lines around 1330 nm (Fig. 10(b) top panel). The additional components shown in Fig. 11(b) resolved by OSA can be identified using known spectroscopic constants as R31, R40, P45, and P47 of ($v' = 32 \rightarrow v'' = 72$) lasing transitions.

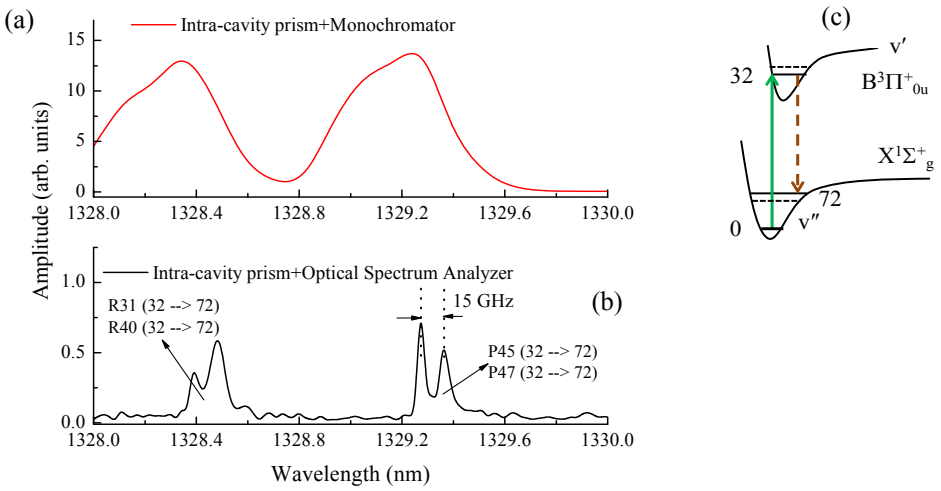

Fig. 11 I_2 laser emission around 1330 nm recorded with a grating spectrometer (resolution 0.5 nm) (a) and optical spectrum analyzer (Thorlabs OSA203B) (b). (c) I_2 simplified energy level schema.

Each of these components may include 15 to 21 hyperfine lines depending on even or odd j″ rotational transition. No attempt was made to resolve the hyperfine structures. The occurrence of these particular R and P transitions indicates fast rot-rot energy transfer.

Polarization Coupling: In order to gain a better understanding of the physics governing the 1.3 μm lasing and possible coherent pump to laser coupling, we have measured polarization dependence of transmitted pump as well as that of I_2 HOFGLAS. For this measurement, a λ/2 plate was used to control the angle of the linear polarization of input pump. At the output of the fiber, the pump transmission was measured as function of polarizer (analyzer) angle, see Fig.12.

It is interesting to note that the fiber rotates the pump polarization by about 90°; the maximum contrast is observed when the input pump polarization state is set at a particular angle with respect to fiber- in our case with the current fiber arrangement, it is about 135°. The overall transmission of the pump did not depend on the input polarization. We thus conclude that the fiber shows birefringence at the pump wavelength.

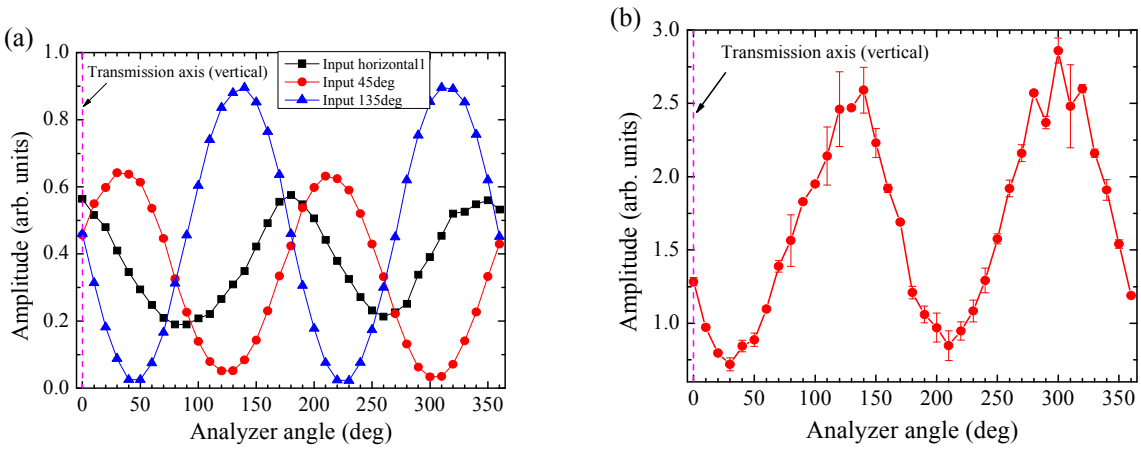

Fig. 12 (a) Transmitted pump (off-resonant, no absorption) as a function of a polarizer (analyzer) angle. 0 degree corresponds to analyzer angle perpendicular to pump polarization if there is no fiber present, (b) output polarization with the pump at 135° and tuned to resonance so that lasing occurs.

I_2 HOFGLAS polarization was recorded at one particular pump polarization state. Figure 12(b) shows the transmitted I_2 HOFGLAS power through the analyzer as a function of analyzer angle. It appears that the laser polarization follows the output pump polarization. The fact that the laser polarization shows a dominant axis points to certain coherent coupling of pump to laser. If the coupling were completely incoherent, the laser is independent of

the phase of the pump field; the laser output would not show a preferred polarization direction. It should be noted that we carefully avoided any polarization selective elements in the cavity. Another reason for the laser having a preferred polarization could be due to fiber having polarization dependent loss at the laser wavelength. This will be explored further. To this end we will measure the fiber transmission as function of polarization using a single-frequency diode laser.

Simultaneous lasing: When pumped at 532 nm, I_2 potentially can lase from ~540-1345 nm. Figure 13 shows an emission spectrum from I_2 filled 80-μm hollow core fiber when excited with 532 nm. The spectrum is well explained with the known Franck-Condon factors for I_2 [3]. We carried out preliminary measurements to demonstrate simultaneous lasing in the visible as well as NIR spectral regions from a I_2 HOFGLAS. The pump laser parameters are the same as in previous measurements. The iodine pressure was kept constant at about 250 mtorr (vapor pressure at room temperature).

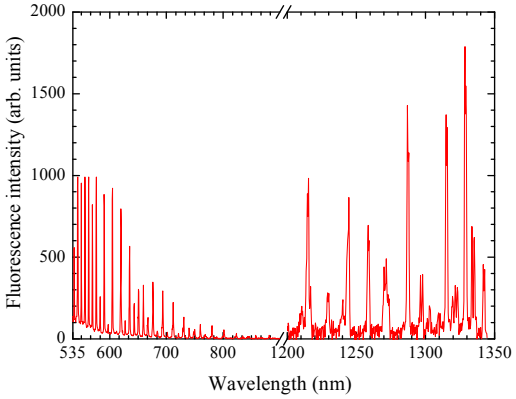

Fig. 13 Measured emission spectrum of I_2 (300 mtorr) when excited at 532 nm (the fluorescence amplitudes in the VIS and NIR are not calibrated relative to each other; they were recorded with different detectors). The fluorescence was collected from the side, through the cell wall and imaged into the spectrometer. The other parameters were similar to those shown in Fig.1. A shutter in front of the outcoupler prevented lasing. Pump power 115 mW.

The hollow core fiber used in these measurements had a loss of ~30 dB/km at the laser emission wavelength region of 1300-1350 nm and relatively large loss of about 42 dB/m at the pump wavelength. Figure 14 compares the fluorescence in the VIS with and without lasing (shutter in front of outcoupler open). Pumping occurred on the v = 0 → v = 32 of the $B^3\Pi^+_{0u} \leftarrow X^1\Sigma^+_g$ electronic transition near 532 nm. When 1.3 μm lasing is turned on, the 540-700 nm emission is not completely suppressed. It drops only by about 15%, indicating that there is still gain available in the visible wavelength band. This suggests the possibility of simultaneous lasing in the near IR and VIS spectral region provided proper choice of mirrors and fiber.

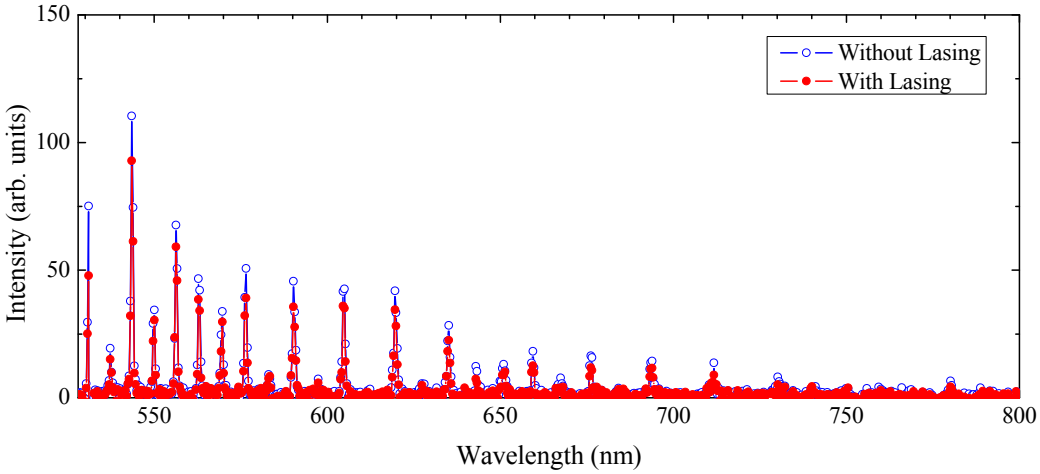

Fig.14 The visible emission spectrum of I_2 HOFGLAS when the 1.3 μm lasing is turned on and when 1.3 μm lasing was inhibited.

E.2. Acetylene HOFGLAS, Kansas State University

We have demonstrated near-diffraction limited performance of an OPA-pumped acetylene-filled HOFGLAS system at the highest pulse energy of 1.4 μJ at 3 μm [4-7]. The HOFGLAS with an inhibited coupling (IC) kagome-structured fiber and a hypocycloidal core of 10.9 m length operates without any saturation at a slope efficiency of ~ 20%. The stable 3-μm output comes with a near-diffraction limited mode quality (M^2 = 1.15) and improved performance over the previous realizations of acetylene-filled HOFGLAS systems in terms of pulse energies and dependence of slope efficiency on pressure. An earlier measure of M^2 is shown below in Fig. 15, where an M_x^2 value of 1.71±0.19 was measured at an average lasing wavelength of 3.1435 μm. More recently, we have improved the measured value of M^2 to below 1.2, and improved the pump energy and hence the mode matching between the OPA pump and the IC kagome fiber.

The total pump pulse energy absorbed by the gas and fiber on resonance with P(13) and R(11) molecular transitions can be obtained by subtracting combined beam power after vacuum chambers from input pump power and adding mid-IR laser power to the result. Corrections for transmission through all BK7 and CaF_2 optics and for coupling efficiency into HC-PCF off resonance have been considered carefully. By continuously varying the incident pump pulse energy via the variable attenuator after the optical parametric amplifier (OPA), the output characteristics of the laser at 3 μm in terms of pump energy absorbed by gas were obtained for each acetylene pressure ranging from 1.2 torr to 14 torr, as shown in Fig.16. (b). A similar curve appearing in Ref. [4] shows slightly smaller quantities on the x-axis. The discrepancy is due to a difference in the way fiber losses are considered. Fig.16 reflects our best understanding of those losses at the present time.

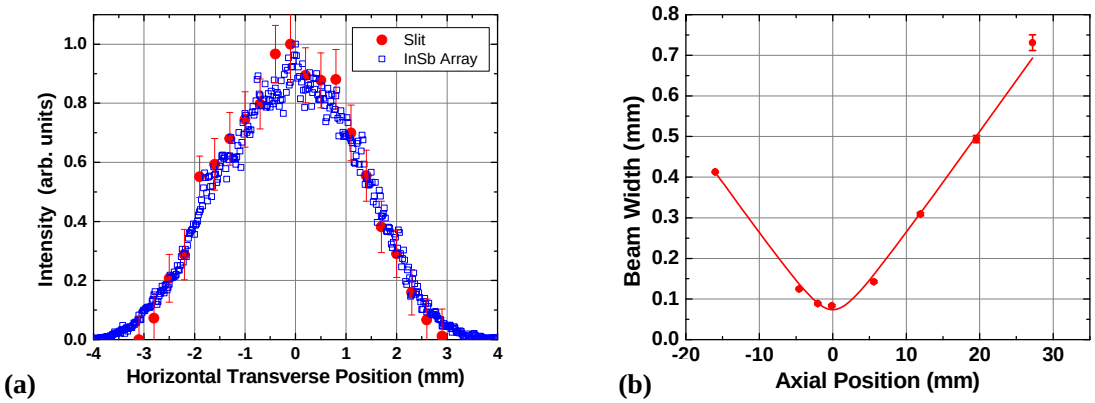

Fig.15. (a) The transverse horizontal beam profile of mid-IR gas laser measured using the scanning slit technique (circles). The output mode of this fiber was also measured by coupling another mid-IR laser into the fiber and imaging the mode onto an InSb array (squares). (b) Plot of beam width as a function of axial position (z).

Apart from the better mode quality, our work here highlights the power scalability and beam quality that can be achieved from a stable OPA-pumped acetylene-filled HOFGLAS configuration. We report the highest 3 μm pulse energy output achieved from an acetylene-filled pulsed HOFGLAS. With a HOFGLAS system comprised of a 10.9 m length of IC kagome fiber filled with acetylene at 9.8 torr, we were able to achieve the maximum 3 μm pulse energy of 1.4 μJ when acetylene absorbed 8.2 μJ of OPA pump pulse energy along the P(13) absorption line at 1.53 μm. To the best of our knowledge, this output laser pulse energy is nearly two times higher than the pulse energy reported in the most recent work [8]. The performance of the laser in terms of the highest 3 μm pulse energy that it can deliver is expected to be higher if we can pump at higher pump pulse energies. Also, the laser operated without any saturation at the output at a nearly constant slope efficiency of ~ 20% with respect to the absorbed pump pulse energy, nearly independent of the acetylene pressure inside the fiber.

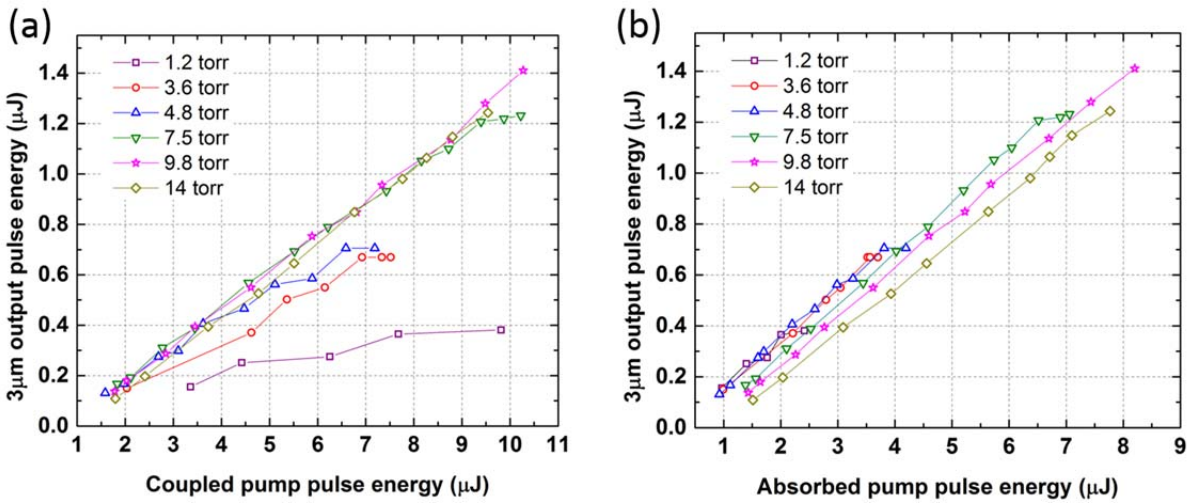

Fig. 16. Laser output pulse energy at 3 μm versus (a) coupled pump pulse energy at 1.53 μm into the fiber with coupling lens of focal length f = 50 mm (b) estimated pump pulse energy absorbed by acetylene.

To quantify the mode quality of the 3 μm laser, we measured M_x^2 by scanning a 20 μm wide slit in the x (transverse) direction to measure multiple beam profiles along the propagation axis (z) of the laser output beam along the focus of a CaF_2 lens, as shown in Fig. 17. The beam widths thus obtained were fitted to obtain M^2 value of the laser output. M^2 values were measured for various 3 μm pulse energies while the HOFGLAS operated with 9.8 torr acetylene pressure and the beam quality stayed uncompromised. Although M^2=1 corresponds to an ideal Gaussian, $M_x^2 < 1.2$ still stands for excellent beam quality and clearly reflects the near-diffraction limited performance of the produced 3 μm output from acetylene HOFGLAS.

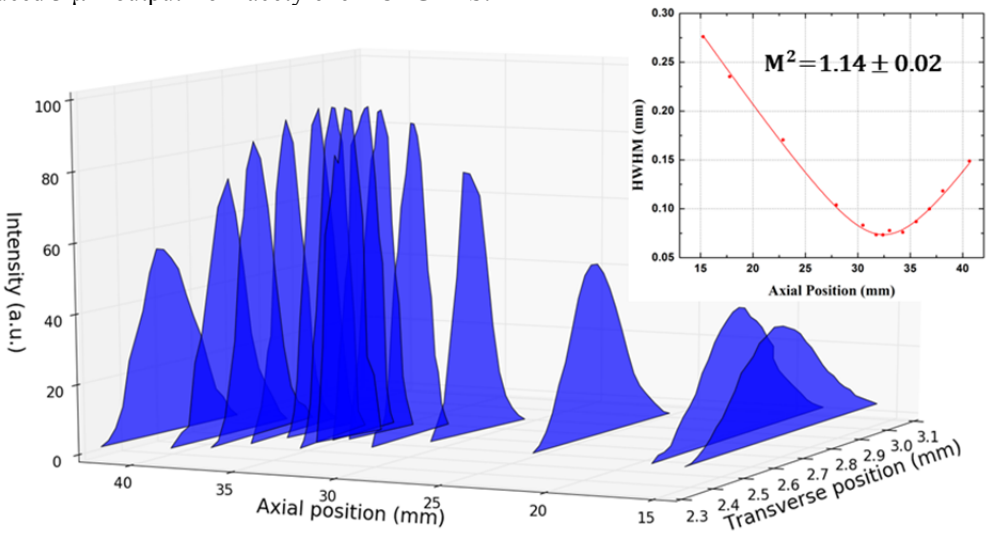

Fig. 17. Cascade plot of beam profiles measured by scanning a 20 μm wide slit across the 3 μm laser output at various axial positions along the beam. Inset shows the beam waist values fitted to the definition of M^2 and average wavelength of output 3.143 μm.

E.3. Ultra-low loss fibers and Raman combs, Xlim, CNRS

Considerable progress was made during this grant period to improve the state of the art in Inhibited-Coupling hollow fibers, particularly in reducing low across the spectrum. Key improvements are summarized below, and the details appear or will appear in publications in the near future.

First, ultra-large band and low loss Kagome fibers (<50 dB/km), with which a near 6-octave Raman comb has been achieved. We stress particularly the remarkable IR coverage of this comb down to a wavelength of 12.7 um. Such fibers are promising for HOFGLAS demonstrations in the infrared. [11]

Secondly, we have pushed the state-of-the art in tubular lattice fiber. Here a fiber with a loss of 7.7 dB/km has been achieved. This is just a factor 2 above the fundamental limit of Rayleigh scattering in silica. With respect to the project aim, such a fiber represents a step change in the performance prospects of the Iodine laser. This tubular lattice fiber also shows a very broad guidance with loss lower than 20dB/km, making the prospect of HOFGLAS even more attractive.

A new record-low loss in Kagome lattice fiber has been demonstrated: 8 dB/km at 1 um. [12] And toward a continuation of this project into novel architectures, parameter space for dual core fiber has been explored for further development of HOFGLAS. This work is not yet published.

E.4. To/Hm fiber lasers, Kansas State University

Toward improvements in measurements of fiber loss, we have demonstrated and improved the state of the art in mode-locked fiber lasers in the 2 μm wavelength region. Specifically during this grant period, we have systematically studied the dispersion compensation required to optimize the performance of these lasers. Stretched-pulse operation of a mode-locked thulium/holmium-doped fiber laser has been demonstrated using a high numerical aperture (NA) fiber inside the laser cavity for intracavity dispersion compensation. The high NA fiber exhibits normal group-velocity dispersion allowing for the net-cavity dispersion to be positive. We experimentally investigate the laser dynamics as a function of the net-cavity dispersion, observing the transition from stretched-pulse to solitonic operation as the length of high NA fiber was reduced. In the stretched-pulse regime the laser produced pulses with a bandwidth of 30 nm and duration of 450 fs. Methods for compensating the third-order dispersion using high NA fibers are proposed [13]. Here, we demonstrate a Tm/Ho doped fiber laser that operated in the stretched-pulse regime that uses a high NA fiber for intracavity dispersion compensation. We show here that we can obtain similar bandwidth as previously reported without the use of any free-space components in the laser cavity.

The passive mode-locking techniques used for erbium or ytterbium lasers can be applied towards Tm/Ho fiber systems. Similar to Er doped fiber lasers, Tm/Ho doped fiber lasers can be mode-locked in the stretched-pulse regime where a wider bandwidth is produced than what is observed when operating in the solitonic regime [14]. Control of the net dispersion in a fiber laser cavity is obtained by using sections of normal and anomalous group-velocity dispersion fiber (GVD) in the cavity. The operation regime depends on the sign of the net-cavity GVD. The formation of solitons in the cavity, which occurs when the net-cavity GVD is negative, limits the output pulse duration, peak power, and pulse energy. In contrast when the net-cavity GVD is small but positive solitons do not form but the intracavity pulse periodically stretches and compresses for each round trip, allowing for the formation of shorter pulses. Achieving a positive net-cavity GVD is challenging for Tm/Ho doped fibers lasers since it is difficult to find fibers with normal GVD at 2 μm to compensate the anomalous GVD of the gain fiber and the Corning SMF-28 single-mode fiber (SMF) in the laser. The normal GVD fiber must have large waveguide dispersion since bulk fused silica has anomalous GVD at 2 μm. Previously, we reported using a highly nonlinear fiber for external compensation showing that it had too small normal GVD to compensate the large anomalous GVD of SMF [15]. Recent work has used high numerical aperture (NA) fibers as normal GVD fibers.

The cavity for the Tm/Ho fiber laser is shown in Fig. 18(a) and its solitonic operation described in [15]. An amplified 1560 nm pump light is coupled in the cavity using 1560/2000 nm wavelength division multiplexer. The high-NA fiber is used as a normal dispersion fiber for intracavity dispersion compensation. When no high-NA fiber was in the cavity the laser operated in a solitonic mode producing pulses 9 nm in bandwidth which can support the transform limited pulse duration of 440 fs. The laser is mode-locked via nonlinear polarization rotation by adjusting the two polarization controllers PC1 and PC2 when pump power is about 300 mW. The spectrum and pulse duration of the laser output are measured by a spectrometer and an interferometric autocorrelator (IAC). All spectral and IAC measurements were performed after 1.0 m of SMF on the laser's output coupler.

Fibers from the family of ultra-high NA (UHNA) fibers manufactured by Nufern were explored as candidate normal GVD fibers [16]. Stretched-pulse operation was observed when the fiber UHNA4 was used inside the cavity. Figure 18(b) shows spectra for both stretched-pulse and solitonic operation. For stretched-pulse operation the pulse duration was 0.45ps assuming a Gaussian pulse shape, compared 1.24 ps for the solitonic operation assuming sech^2 pulse shape. The ratio of pulse width to IAC width was computed to be 0.590 and 0.527 for Gaussian and sech^2 respectively.

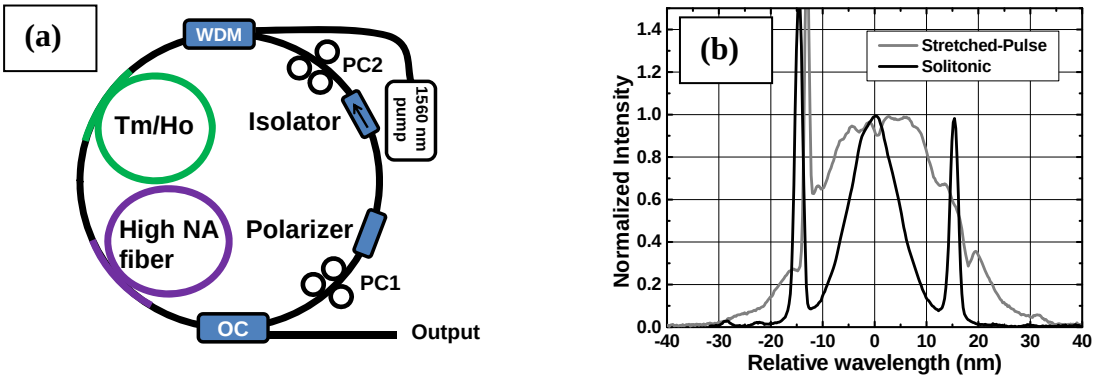

Fig. 18 (a) The mode-locked Tm/Ho fiber laser: WDM, wavelength division multiplexor; OC, output coupler; PC, polarization controller. The laser operated in stretch pulse mode with the high NA fiber and solitonic mode without the high NA fiber. (b) Output spectra of the laser in stretched-pulse (gray) and solitonic (black) operation for a UHNA4 length of 2.35 m. The center wavelengths were 1960 nm and 1940 nm in solitonic and stretched-pulse regimes respectively.

F. References

[1] V. A. Nampoothiri, W. Rudolph, B. Debord, M. M. Alharbi, F. Gérôme, and F. Benabid, "CW Hollow Core Optically Pumped Fiber Gas Laser," in CLEO: 2014, OSA Technical Digest (online) (Optical Society of America, 2014), paper SM3N.3. http://www.opticsinfobase.org/abstract.cfm?URI=CLEO_SI-2014-SM3N.3

[2] "CW Hollow Core Optically Pumped I_2 Fiber Gas Laser", A. V. V. Nampoothiri, B. Debord, M. Alharbi, F. Gérôme, F. Benabid, and W. Rudolph, Opt. Lett. **40**, 605-608 (2015). doi:10.1364/OL.40.000605

[3] Martin, F., Bacis, R., Churassy, S. and Verges, J., "Laser-induced-fluorescence Fourier transform spectrometry of the XO_g^+ state of I_2: Extensive analysis of the $BO_u^+ \rightarrow XO_g^+$ fluorescence spectrum of $^{127}I_2$". Journal of Molecular Spectroscopy, **116,** (1986), pp.71-100.

[4] N. Dadashzadeh, M. Thirugnanasambandam, K. Weerasinghe, B. Debord, M. Chafer, F. Gérôme, F. Benabid, B. Washburn, and K. Corwin, "Power-scaling a Mid-IR OPA-pumped Acetylene-filled Hollow-Core Photonic Crystal Fiber Laser," in *Conference on Lasers and Electro-Optics*, OSA Technical Digest (2016) (Optical Society of America, 2016), paper STh4O.1. https://doi.org/10.1364/CLEO_SI.2016.STh4O.1

[5] N. Dadashzadeh, M. Thirugnanasambandam, K. Weerasinghe, B. Debord, M. Chafer, F. Gérôme, F. Benabid, B. Washburn, and K. L. Corwin, "Near-Gaussian Spatial Mode from a Mid-IR Acetylene-filled Hollow-Core Fiber Laser," in *Frontiers in Optics 2016*, OSA Technical Digest (online) (Optical Society of America, 2016), paper FTu1I.5. https://doi.org/10.1364/FIO.2016.FTu1I.5

[6] N. Dadashzadeh, K. Weerasinghe, A. Jones, B. Debord, F. Gerome, F. Benabid, B. Washburn, and K. Corwin, "Mode Profile of a Mid-IR Gas-filled Hollow-Core Photonic Crystal Fiber Laser," in *Frontiers in Optics 2015*, OSA Technical Digest (online) (Optical Society of America, 2015), paper LTh4I.4. https://doi.org/10.1364/LS.2015.LTh4I.4

[7] N. Dadashzadeh, M. P. Thirugnanasambandam, K. Weerasinghe, B. Debord, M. Chafer, F. Gerome, F. Benabid, B. R. Washburn and K. L. Corwin, "High energy, near diffraction-limited performance of OPA pumped Acetylene-filled Hollow-core Optical Fiber Gas Laser in mid-IR," *in preparation.*

[8] Z. Wang, W. Belardi, F. Yu, W. J. Wadsworth, and J. C. Knight, "Efficient diode-pumped mid-infrared emission from acetylene-filled hollow-core fiber," Opt. Express **22**(18): 21872-8 (2014).

[9] M. Abu Hassan, F. Yu, W. Wadsworth, and J. Knight, "Cavity-based mid-IR fiber gas laser pumped by a diode laser," Optica 3, 218-221 (2016).

[10] A. Benoit, B. Beaudou, M. Alharbi, B. Debord, F. Gerome, F. Salin, and F. Benabid, " Over-five octaves wide Raman combs in high-power picosecond-laser pumped H_2-filled inhibited-coupling Kagome fiber", Optics Express **23**(11) 14002-14009 (2015).

[11] B. Debord, A. Amsanpally, M. Chafer, A. Baz, M. Maurel, J.-M. Blondy, E. Hugonnot, F. Schol, Vincetti, F. Gérôme, and F. Benabid, "Ultralow transmission loss in inhibited-coupling guiding hollow fibers," Optica, *accepted,* (2017).

[12] DEBORD B., MAUREL M., AMSANPALLY A., ADNAN M., BEAUDOU B., BLONDY J.-M., VINCETTI L., GÉRÔME F., BENABID F.: "Ultra-low loss (8.5 dB/km @ Yb-laser region) inhibited-coupling Kagome HC-PCF for laser beam delivery applications" , Photonic West, Paper 10094-58, San Francisco, California, 28 January - 2 February 2017.

[13] R. Kadel and B. R. Washburn, "Stretched-Pulse and Solitonic Operation of an All-Fiber Thulium/Holmium

Doped Fiber Laser," Appl. Opt. **54**, 746-750 (2015).

[14] H. A. Haus, K. Tamura, L. E. Nelson, and E. P. Ippen, "Structure-pulse additive pulse mode-locking in fiber ring laser: Theory and experiment," *IEEE J. of Quantum Electron.*, vol. 31, p.591-598(1995).

[15] R. Kadel and B. R. Washburn, "An all fiber mode-locked Tm/Ho fiber laser employing c-band components," in *in Frontiers in Optics (FiO)*, San Jose, paper FTul3 (2011).

[16] Nufern UHNA series of fibers*http://www.nufern.com/pam/optical_fibers/983/UHNA1/*.